Chapter 10

Multivariate Mathematical Morphology applied to Color Image Analysis

10.1. Introduction

Mathematical morphology (MM) theory, founded by G. Matheron [MAT 75] and J. Serra [SER 82], is a powerful image analysis framework, currently fully developed for both binary and gray-level images. Its popularity in the image processing community is mainly due to its rigorous mathematical foundation as well as its inherent ability to exploit the spatial relationships of pixels. The morphological framework provides a rich set of tools able to perform from the simplest to the most demanding tasks: noise reduction, edge detection, segmentation, texture and shape analysis, etc. As a methodology, it has been applied to almost all application areas dealing with digital image processing [SOI 03]. Consequently, it was only a matter of time before attempting to extend the same concepts to color and more generally to multivalued images, i.e. images with more than one channel.

This extension is not straightforward, however. Specifically, the morphological framework is based on complete lattices [HEI 94]. In order to accommodate multivalued images, a way of calculating the extrema of vector data is essential. However, unlike scalars, there is no unambiguous way of ordering vectors. Even if most of the known vector ordering schemes have already been employed for defining multivariate morphological operators, none of them has yet been widely accepted.

Chapter written by E. APTOULA and S. LEFÈVRE.

The lexicographical ordering is certainly the most commonly adopted choice due to its positive theoretical properties, totality and antisymmetry, in combination with its inherent capacity for flexible ordering configurations. However, this ordering comes with the severe drawback that the level of priority attributed to the first vector dimension during lexicographical comparison greatly hinders the effective exploitation of the subsequent image channels.

The existence of balanced lexicographical orderings provides new ways to build theoretically sound and practically relevant multivariate morphological operators. Such operators can then be involved in any mutivariate image processing task, e.g. filtering, segmentation or classification.

10.1.1. *Chapter organization*

This chapter initially provides an overview of the theoretical background of multivariate morphology and of the main available color spaces (section 10.2), and then continues to elaborate on the existing approaches used for extending the fundamental operators of MM to multivariate data (section 10.3). That is why cases limited only to specific operators have been omitted (e.g. color image segmentation). As one of our primary purposes is to present the state-of-the-art in color morphology, we focus particularly on cases developed with color images in mind. Nevertheless, the scope of the survey is not limited to color-specific vector ordering approaches, since theoretically an ordering is independent of the represented context (e.g. a color, a multispectral pixel value, etc). That is why morphological solutions that have been developed for non-color data, but can however be trivially applied to this case, are also included. Due to their rich diversity and overwhelming number, they are examined according to their methodology of ordering their multivalued input.

The problematic aspect of lexicographical ordering is dealt with in section 10.4, where we review in great detail the existing solutions as well as their practical limits. In particular, new ways of modifying lexicographical ordering for increased symmetry among its components will be presented, including an approach leading to pseudo-morphological operators.

Finally we proceed to an application-oriented comparative study of the major approaches (section 10.5). We conduct tests in color image analysis with the aim of texture classification. The goal here is to compare the performance of different vector ordering schemes as a basis for morphological operators, and to assert their theoretical properties with the help of experimental results.

10.2. Extension of mathematical morphology to multivariate data

In this section we briefly recall the theoretical concepts behind the extension of morphological operators to multivariate images. For an in-depth study of the theory behind multivariate mathematical morphology, refer to [GOU 95, SER 93]. A brief introduction to main color spaces is also given.

10.2.1. *Orderings and lattices*

As the concept of order plays a central role in this field, we start by recalling the relative definitions. A binary relation $\mathcal{R}$ on a set $\mathcal{S}$ is called:

– *reflexive* if $x \mathcal{R} x, \ \forall x \in \mathcal{S}$;

– *antisymmetric* if $x \mathcal{R} y$ and $y \mathcal{R} x \Rightarrow x = y, \ \forall x, y \in \mathcal{S}$;

– *transitive* if $x \mathcal{R} y$ and $y \mathcal{R} w \Rightarrow x \mathcal{R} w, \ \forall x, y, w \in \mathcal{S}$ or

– *total* if $x \mathcal{R} y$ or $y \mathcal{R} x, \ \forall x, y \in \mathcal{S}$.

A binary relation $\leq$ that is reflexive and transitive is called a *pre-ordering* (or *quasi-ordering*); if the antisymmetry constraint is also met, it becomes an *ordering*. In addition, if the totality statement holds for $\leq$ it is denoted as *total*; if it does not hold it is referred to as *partial*.

The complete lattice theory is widely accepted as the appropriate algebraic basis for mathematical morphology [RON 91]. As well as unifying the approaches previously employed in binary and gray-level morphology, it also makes it possible to generalize the fundamental concepts of morphological operators to a wider variety of image types and situations.

Specifically, a *complete lattice* $\mathcal{L}$ is a non-empty set equipped with a partial ordering $\leq$, such that every non-empty subset $\mathcal{P}$ of $\mathcal{L}$ has a greatest lower bound $\bigwedge \mathcal{P}$ called *infimum* and a least upper bound $\bigvee \mathcal{P}$ called *supremum*. In this context, images are modeled by functions mapping their domain space $\mathcal{E}$, an arbitrary non-empty set that is an abelian group with respect to $+$, into a complete lattice $\mathcal{T}$ (with $\top$ and $\bot$ its greatest and least elements, respectively), defining the set of possible gray values. Moreover, if $\mathcal{F}$ represents the set of functions $f : \mathcal{E} \rightarrow \mathcal{T}$, then for the partial ordering:

$$f, g : \mathcal{E} \rightarrow \mathcal{T}, \ \ f \leq g \Leftrightarrow \forall x \in \mathcal{E}, \ \ f(x) \leq g(x). \tag{10.1}$$

$\mathcal{F}$ also forms a complete lattice, where $f(x) \leq g(x)$ refers to the partial ordering in $\mathcal{T}$. In other words, a complete lattice structure is imposed on the pixel intensity range. Usually $\mathcal{E}$ (the space of pixels) is taken to be either $\mathbb{R}^d$ (d-dimensional Euclidean space) or $\mathbb{Z}^d$ (d-dimensional discrete space); $\mathcal{F}$ therefore corresponds to the set of

continuous or discrete images, respectively. Likewise, various choices are available for $\mathcal{T}$, such as $\mathcal{T} = \overline{\mathbb{R}}^n$ ($\overline{\mathbb{R}} = \mathbb{R} \cup \{+\infty, -\infty\}$) and $\mathcal{T} = \overline{\mathbb{Z}}^n$. The case of $n > 1$ corresponds to the so-called multivalued images [GOU 00], while $n = 3$ specifically includes color images. Namely, in the case of a multivalued image with n components, $\mathcal{T} = \mathcal{T}_1 \times \ldots \times \mathcal{T}_n$ is considered as the Cartesian product of n complete lattices. Each mapping $f_i : \mathcal{E} \rightarrow \mathcal{T}_i, \ \ i \in \{1, \ldots, n\}$ is called a *channel* or *band* of the multivalued image.

Within this model, morphological operators are represented by mappings between complete lattices (i.e. the input and output images) with some additional properties such as increasingness and translation invariance. They are employed in combination with matching patterns, called *structuring elements* (SE), that are usually subsets of $\mathcal{E}$ (i.e. *flat* SE). Particularly, *erosion* and *dilation* constitute the fundamental blocks of MM, from the combinations of which several sophisticated operators can be derived. More precisely, from an algebraic point of view, given two complete lattices $\mathcal{L}$ and $\mathcal{M}$ an operator $\varepsilon : \mathcal{L} \rightarrow \mathcal{M}$ is called an erosion if it is distributive over infima. In other words, $\varepsilon(\bigwedge_i P_i) = \bigwedge_i \varepsilon(P_i)$ for every collection $\{P_i\}$ of elements of $\mathcal{L}$. Similarly, $\delta : \mathcal{L} \rightarrow \mathcal{M}$ is called a dilation if it is distributive over suprema, i.e. $\delta(\bigvee_i P_i) = \bigvee_i \delta(P_i)$ for every collection $\{P_i\}$ of elements of $\mathcal{L}$. As suggested in [SER 82], dilation and erosion basically rely on three concepts: a ranking scheme, the extrema derived from this ranking and finally the possibility of admitting an infinity of operands. However, the former two are missing from multivalued images.

For example, if we apply the preceding notions to the case of continuous multidimensional gray-level images ($f : \mathbb{R}^d \rightarrow \overline{\mathbb{R}}$), it suffices to replace the partial ordering $\leq$ of $\mathcal{T}$ with the usual comparison operator in $\overline{\mathbb{R}}$, in order to induce a complete lattice structure on $\mathcal{T}$ and subsequently on $\mathcal{F}$ by means of equation (10.1), which will make the computation of extrema possible during erosion and dilation. Likewise, the inclusion operator $\subseteq$ can be used with binary images ($f : \mathbb{R}^d \rightarrow \{0, 1\}$). However, if we now consider multivalued images ($f : \mathbb{R}^d \rightarrow \overline{\mathbb{R}}^n, \ \ n > 1$), it becomes problematic to find an ordering relation for the vectors of $\overline{\mathbb{R}}^n$, due to the fact that there is no universal method for ordering multivariate data.

In order to remedy this inconvenience, Goutsias *et al.* [GOU 95] proposed employing an adequate surjective mapping h to transform the image data into a more suitable space for morphological operators. More precisely, the idea of using a surjective mapping $h : \mathcal{T} \rightarrow \mathcal{L}$, where $\mathcal{T}$ is a non-empty set and $\mathcal{L}$ a complete lattice, constitutes the theoretical support upon which several of the present multivariate morphological frameworks are based. Specifically, its importance lies in the fact that $\mathcal{T}$ is no longer required to be a complete lattice, since the ordering of $\mathcal{L}$ can be induced upon $\mathcal{T}$ by means of h:

$$\forall\, t, t' \in \mathcal{T}, \ \ t \leq_h t' \Leftrightarrow h(t) \leq h(t') \tag{10.2}$$

hence making it possible to construct h-morphological operators on $\mathcal{T}$. Consequently, we can deal with multivalued images $f : \mathcal{E} \rightarrow \mathbb{R}^n$ through the use of a well-chosen mapping $h : \mathbb{R}^n \rightarrow \mathcal{L}$, where $\mathcal{L}$ is a new, more suitable space for lattice-based operations [GOU 95, GOU 00].

In addition, given an adequate vector ranking scheme, the vector erosion (ε_b) and dilation (δ_b) of a multivalued image $\mathbf{f}$ by a flat SE b can be expressed by means of the vector extrema operators $\sup_v$ and $\inf_v$ based on the given ordering:

$$\varepsilon_b(\mathbf{f})(\mathbf{x}) = \inf_{\mathbf{s} \in b}{}_v \{\mathbf{f}(\mathbf{x} + \mathbf{s})\}, \tag{10.3}$$

$$\delta_b(\mathbf{f})(\mathbf{x}) = \sup_{\mathbf{s} \in b}{}_v \{\mathbf{f}(\mathbf{x} - \mathbf{s})\}. \tag{10.4}$$

The main obstacle preventing the extension of morphological operators to multivalued images therefore consists of defining an ordering relation that will induce a complete lattice structure on the set of vector pixel intensities.

10.2.2. *Color spaces*

A rich number of color specification and visualization methods or *color spaces* are currently available. While some were designed and developed with a certain family of applications in mind, others were conceived as general-purpose color representations. Each color space has its own set of desirable properties as well as drawbacks for purposes of color image processing and computer vision. Our goal is not to provide a complete overview of the principal color spaces, but to focus on those which will be discussed and used throughout this chapter.

10.2.2.1. *Red, green, blue*

Red, green, blue (RGB) is by far the most widely used color space in imaging environments. It can be found in televisions, computer monitors and digital cameras, among others. Theoretically, it is based on the concept of trichromaticity and on the reference color-matching functions defined by the *Commission Internationale de l'Eclairage* (CIE); it therefore represents colors as combinations of the three primaries. Specifically, it is considered as an *additive* color model. In additive color reproduction, the mixing of primary colors with the purpose of obtaining secondary colors is realized on the basis of light emission. Conversely, in subtractive models light reflection is taken as a reference. Consequently, combining for instance red and green leads to yellow ($R = \max, G = \max, B = 0$), whereas red and blue gives magenta ($R = \max, G = 0, B = \max$). Black is considered as the absence of light, hence no primary color is necessary for its production ($R = G = B = 0$). White, on the

other hand, is equivalent to the presence of all primary colors in maximal amounts ($R = G = B = \max$).

Despite its widespread use, however, RGB suffers from multiple inconveniences. First, with the exception of the eight cube corners, it is intuitively difficult to specify arbitrary colors by means of the RGB cube. Furthermore, the distances between points residing inside the cube are not proportional to their perceptual differences; in other words, RGB is perceptually non-uniform. Additionally, the exact values of the R, G and B components of a given color depend on the spectral sensitivity functions of the acquisition device under consideration, hence rendering this space device dependent. Finally, the three components of RGB are highly correlated; specifically, $\rho_{BR} = 0.78$, $\rho_{RG} = 0.98$ and $\rho_{GB} = 0.94$. Due to these drawbacks, RGB has generally been considered as an unsuitable color space for digital image processing.

10.2.2.2. *Perceptually uniform color spaces*

Perceptual uniformity, the property which for a change of color value induces a perceptually proportional change, has been a long-desired property of color spaces. As this invaluable property for computing color differences was not provided by the initial XYZ color space, in 1976 CIE adopted both CIELAB (or L*a*b*) and CIELUV (or L*u*v*), when no consensus could be achieved over one or the other. Both of these spaces are considered almost perceptually uniform or linear (for small values) and are derived from XYZ. Given an image produced by an acquisition device in RGB, it is necessary to be able to convert it into and from XYZ, i.e.

$$\begin{bmatrix} X & Y & Z \end{bmatrix}^T = A \begin{bmatrix} R & G & B \end{bmatrix}^T \tag{10.5}$$

where the RGB values are normalized to $[0, 1]$ and the matrix A used for this purpose depends on the reference white point corresponding to the illuminant under consideration. For instance, for the widely popular D65 or daylight illuminant, it becomes:

$$A_{D65} = \begin{bmatrix} 0.412 & 0.358 & 0.180 \\ 0.212 & 0.716 & 0.072 \\ 0.019 & 0.119 & 0.950 \end{bmatrix}. \tag{10.6}$$

As both L*a*b* and L*u*v* follow the same principles, we focus solely on L*a*b* where the $L^* \in [0, 100]$ component denotes lightness, a^* the red-green and b^* the yellow-blue opposition. Thus, a^* and b^* possess negative values when the color they represent is close to green and blue, respectively, and positive values when it is closer to red and yellow, respectively. Given the XYZ triplet, the corresponding L*a*b*

representation may be obtained as follows:

$$\begin{aligned} L^* &= 116 f\left(\frac{Y}{Y_n}\right) - 16 \\ a^* &= 500\left[f\left(\frac{X}{X_n}\right) - f\left(\frac{Y}{Y_n}\right)\right] \\ b^* &= 200\left[f\left(\frac{Y}{Y_n}\right) - f\left(\frac{Z}{Z_n}\right)\right] \\ f(t) &= \begin{cases} t^{1/3} \text{ if } t > 0.008856 \\ 7.787t + \frac{16}{116} \text{ otherwise} \end{cases} \end{aligned} \tag{10.7}$$

where X_n, Y_n, Z_n denote the XYZ triplet representing the white point ($R = G = B = 1$), obtained from equation (10.6). Consequently, $L^*a^*b^*$ inherits the white point reference used in the previous XYZ expression. The capacity to compute perceptual color differences is considered to be one of the major advantages of $L^*a^*b^*$ that has been exploited in various color image applications, requiring device independence and/or perceptual uniformity. On the other hand, it has also recently been argued that even though perceptual uniformity is a highly desirable property for color definition and description, its use in the context of image processing is limited since images are not processed in terms of 'perceived values' [SER 05]. Moreover, we cannot benefit from the property of device independence in cases where no *a priori* information is available on the acquisition conditions of the images under consideration. Additionally, the transformations to and from RGB become computationally complex with the intermediate role of XYZ, hence the practical interest of $L^*a^*b^*$ has been considerably limited in real-time applications.

10.2.2.3. *Phenomenal color spaces*

Phenomenal or polar color spaces are those that express colors in intuitive terms as far as human observers are concerned. Here, color is separated into the following notions:

– *Hue*: represents the dominant wavelength of a color, described as green, blue, etc. It is an angular, modulo 2π value $H \in [0, 2\pi] = [0°, 360°]$, with $0°$ corresponding to red.

– *Saturation* ($S \in [0, 1]$): describes the purity of a color. A fully saturated color appears vivid, whereas zero saturation transforms it into a shade of gray. Saturation can therefore also be considered as the distance from the achromatic axis.

– *Brightness*, *luminance* or *value* (L): denotes the component describing the sensation associated with the amount of emitted light, or in other words the amplitude of the color under consideration. Similarly to saturation, it is often normalized to $[0, 1]$.

Polar spaces in their majority are obtained through direct transformations from RGB, hence being perceptually non-uniform and device dependent. An additional

disadvantage that further hinders their use (apart from color specification) is the angular nature of hue, which through modulo-based operations leads to visual discontinuities. Moreover, the most widely used representatives of this category (HSV and HLS) suffer from major structural inconveniences [HAN 08]. For these reasons, phenomenal spaces have long been viewed as unsuitable for color image processing. Indeed, they lack the properties of independence of saturation from brightness, existence of norms for the notions of brightness and saturation and inversibility of the space back to RGB. Some recent original phenomenal spaces have therefore been proposed, e.g. LSH [ANG 05] which is defined from RGB as:

$$\begin{aligned} L_{\mathrm{LSH}} &= \frac{1}{3}(\max + \mathrm{med} + \min) \\ S_{\mathrm{LSH}} &= \begin{cases} \frac{3}{2}(\max - L_{\mathrm{LSH}}) & \text{if } L_{\mathrm{LSH}} \geq \mathrm{med} \\ \frac{3}{2}(L_{\mathrm{LSH}} - \min) & \text{if } L_{\mathrm{LSH}} \leq \mathrm{med} \end{cases} \\ H_{\mathrm{LSH}} &= k\left[\lambda + \frac{1}{2} - (-1)^{\lambda}\left(\frac{\max + \min - 2\mathrm{med}}{2S_{\mathrm{LSH}}}\right)\right] \end{aligned} \tag{10.8}$$

where $\max$, med and $\min$ denote the maximum, median and minimum value of the transformed RGB triplet, respectively. k is the angle unit ($\pi/3$ for radians and 42 for 256 levels), whereas λ is set to 0 if $r > g \geq b$, 1 if $g \geq r > b$, 2 if $g > b \geq r$, 3 if $b \geq g > r$, 4 if $b > r \geq g$ and 5 if $r \geq b > g$.

Let us note that the optimal color space choice clearly depends on the needs of the application under consideration. In this chapter, we will not deal further with this issue and instead focus on the ways mathematical morphology can be applied to multivariate images. When dealing with color images. we will mainly illustrate our proposals using the LSH space [ANG 05]. Nevertheless, the proposed solutions for multivariate mathematical morphology are of course not limited to this color space and can be used with any available data representation model.

10.3. Taxonomy of vector orderings

There are two methods for morphological processing of mutivariate images: *marginal* (or *componentwise/scalar*) and *vector*. While marginal processing consists of dealing separately with each channel of the image (completely ignoring the interchannel correlation), vector processing considers all available channels globally and simultaneously but requires the existing algorithms to be adapted in order to accommodate vector data. Much effort has therefore been put into engineering a way of ordering vectors, especially in the last few decades. In this section we review the main solutions proposed in the literature and discuss their advantages and disadvantages. For a more complete survey of this topic, the reader is refered to [APT 07].

Several taxonomies can be given for presenting vectorial orderings, the most famous one being introduced by Barnett [BAR 76] where four different groups are defined. Marginal orderings (M-orderings) correspond to univariate orderings realized on every component of the given vectors, where data are ordered along each one of its channels independently from others, hence the name componentwise ordering.

In conditional orderings (C-orderings), vectors are ordered by means of some of their marginal components and selected sequentially according to different conditions. The components not participating in the comparison process are listed according to the position of their ranked counterparts. Hence, the ordering of the vectors is conditioned upon the particular marginal set of ranked components. Lexicographical ordering constitutes a widely known example of C-ordering, potentially employing all the available components of the given vectors and will be discussed further in this chapter. Let us observe that C-orderings are most suitable for cases where we can establish a priority among the image channels.

Partial orderings (P-orderings) consist of approaches that partition the given vectors into equivalence classes with respect to order, rank or extremeness. They are generally geometric in nature and account for the interrelations between components. Let us remark however that 'partial' is an abuse of terminology (section 10.2) because there are not only total pre-orderings belonging to this class, but algebraically partial orderings do not necessarily belong to this class either. That is why we will employ the term P-ordering.

Finally, reduced orderings (R-orderings) aim to first reduce vectors to scalar values and then rank vectors according to their natural scalar order. A further categorization of R-orderings consists of classifying them as distance orderings and projection orderings. For instance, an R-ordering on $\mathbb{R}^n$ could consist of defining first a transformation $h : \mathbb{R}^n \rightarrow \mathbb{R}$ and then ordering the vectors of $\mathbb{R}^n$ with respect to the scalar order of their projection on $\mathbb{R}$ by h.

According to the chosen transformation, it is possible to obtain a total pre-ordering (h non-injective) or even a total ordering (h injective) [CHA 98]. An additional advantage of R-orderings lies in the fact that with an adequately chosen h, they can attribute equal priority to all components (unlike C-orderings).

In this section, we adopt the scheme employed by Chanussot [CHA 98] where vector orderings are classified according to their algebraic properties (antisymmetry, totality, etc.) and distinguish between partial orderings, total pre-orderings and total orderings. This choice was made with the aim of highlighting the effect that these basic properties have on the end result of processing. Additionally, the vectors of the ordering relations that are mentioned in the following are considered in $\mathbb{R}^3$, unless otherwise specified.

10.3.1. *Partial orderings*

The so-called *marginal* processing strategy, despite usually being presented as an alternative to *vector*, is simply its variant, as it employs the partial ordering defined as

$$\forall \mathbf{v}, \mathbf{v}' \in \mathbb{R}^n, \;\; \mathbf{v} \leq \mathbf{v}' \Leftrightarrow \forall\, i \in \{1, \ldots, n\}\,, \;\; v_i \leq v'_i. \tag{10.9}$$

Obviously, there can be vectors that may not be comparable under this ordering relation, e.g. $\mathbf{a} = [7, 2]^T$ and $\mathbf{b} = [3, 4]^T$. Nevertheless, this does not prevent the definition of valid morphological operators based on extrema computed by means of this ordering [SER 93]. Furthermore, it makes it possible to employ all tools offered by gray-level morphology with no need for special adaptation steps. For instance, the erosion and dilation expressions given in section 10.2 become equivalent to:

$$\boldsymbol{\varepsilon}_b(\mathbf{f})(\mathbf{x}) = [\varepsilon_b(f_1)(\mathbf{x}), \ldots, \varepsilon_b(f_n)(\mathbf{x})]^T \tag{10.10}$$

$$\boldsymbol{\delta}_b(\mathbf{f})(\mathbf{x}) = [\delta_b(f_1)(\mathbf{x}), \ldots, \delta_b(f_n)(\mathbf{x})]^T \tag{10.11}$$

where ε_b and δ_b denote the scalar erosion and dilation operators, respectively, with a SE b. Note that a generalization of the marginal approach was given by the matrix morphology theory of Wilson [WIL 92], which was based on the work of Heijmans and Ronse [HEI 90].

Despite its implementational simplicity, marginal ordering suffers mainly from two disadvantages: not accounting for interchannel information as well as the risk of altering the spectral composition of its input. More precisely, as each component is processed independently, any eventual correlation among them is totally ignored, hence rendering this approach unsuitable for images with highly correlated components (e.g. RGB color images) [AST 90]. A possible solution to this problem, as proposed in [GOU 95], consists of applying a decorrelating transformation (e.g. maximum noise fraction transform (MNF), principal component analysis (PCA), discrete cosine transform, a color space with independent components, etc.) prior to ordering. Nevertheless, these decorrelating transformations also introduce an additional computational burden.

Furthermore, there is absolutely no guarantee that marginally processed vectors belong to the input image. The lack of vector preservation constitutes an undesirable effect for several applications. For example, in the case of color image processing this would lead to the appearance of new hues (also known as *false colors*), deteriorating the visual quality of the result and in particular the color balance and the object boundaries. The effect near the spatial edges leads to the so-called *edge jitter*. This effect is illustrated in Figure 10.1, where the application of a marginal median filter

Figure 10.1. *Example of false colors. From left to right: the original image, the result of a marginal and of a vector (lexicographical) median filter*

leads to the appearance of yellow, as the result of additive combination of red and green.

According to [TAL 98], the only way to use morphological operators without generating new vectors is to impose an order on the vector space by means of a (pre-) ordering verifying the totality constraint. This is why the majority of the published articles on multivalued morphology deal with total (pre-) orderings. However, vector preserving approaches are at the same time limited by this property, due to the restriction imposed on their output (i.e. the output must be a vector from the input set). The marginal approach, however, has access to a much broader range of output values, an advantage which may become valuable during noise reduction [COM 99].

Further attempts motivated by the intuitiveness of the marginal approach have resulted in improvements, and we can cite for instance the work of Al-Otum [ALO 03] who proposes the corrected componentwise morphological algorithm with the goal of preventing the appearance of new vectors. It consists of replacing each new vector of the output with its closest vector from the original image, chosen with the help of a Mahalanobis distance-based error function.

In brief, either accompanied by additional transformations or not, the marginal processing strategy uses conventional gray-level operators and pixels are still treated as scalar values, whereas its potential with color data is severely limited by its lack of vector (or color) preservation.

10.3.2. *Total pre-orderings*

Contrary to the marginal approach by means of the additional property of totality, all vectors become comparable. As a result, it is possible to construct a totally ordered lattice structure. Pixels can therefore be manipulated as whole vectors, and consequently the risk of introducing new vectors is completely eliminated [TAL 98].

All pre-orderings share a common drawback, however, which is the relaxation of the antisymmetry constraint. Distinct vectors can therefore eventually become

equivalent. That is why additional measures become necessary, in order to resolve the ambiguity of eventually multiple extrema. A useful solution, though partial, was proposed by Comer and Delp [COM 99] for this problem. It consists of selecting the output vector according to its position in the SE. In addition, the combination of an adequately chosen pre-ordering with an ordering for tie-breaking purposes has also been successfully used in practice [ANG 07].

10.3.2.1. *Reduced total pre-orderings*

Total pre-orderings can be obtained with R-orderings, employing a non-injective reduction transformation [CHA 98]. Distance measures are typical examples of such transformations; in fact, they account for the majority of the proposed R-orderings. Color distances do not necessarily represent the corresponding perceptual differences, however, unless they are chosen in combination with a perceptually linear color space. That is why distance-based color orderings may lead to unexpected results if used with non-perceptually uniform spaces.

This first variant ranks vectors according to their distance from a reference vector $\mathbf{v}_{\mathrm{ref}}$:

$$\mathbf{v} \leq \mathbf{v}' \Leftrightarrow d(\mathbf{v}, \mathbf{v}_{\mathrm{ref}}) \leq d(\mathbf{v}', \mathbf{v}_{\mathrm{ref}}) \tag{10.12}$$

where $d(\cdot, \cdot)$ represents a distance measure. This particular case of distance-based color ordering has been studied in particular by Angulo [ANG 07], where the pitfall of multiple extrema is avoided by combining the distance computation with the lexicographical cascade (equation (10.17)):

$$\mathbf{v} \leq \mathbf{v}' \Leftrightarrow [d(\mathbf{v}, \mathbf{v}_{\mathrm{ref}}), v_1, \ldots, v_n]^T \leq_L [d(\mathbf{v}', \mathbf{v}_{\mathrm{ref}}), v'_1, \ldots, v'_n]^T . \tag{10.13}$$

If the reference vector is the origin, equation (10.12) becomes equivalent to using the norms of the vectors. A variant of equation (10.12) which eliminates the need for a reference vector, proposed for the morphological processing of multispectral remote sensing data [PLA 04], consists of associating each vector with the sum of its distances from the other vectors of a family $\{\mathbf{v}_j\}$:

$$\forall\, \mathbf{v}_k, \mathbf{v}_l \in \{\mathbf{v}_j\}\,, \;\; \mathbf{v}_k \leq \mathbf{v}_l \Leftrightarrow \sum_j d(\mathbf{v}_k, \mathbf{v}_j) \leq \sum_j d(\mathbf{v}_l, \mathbf{v}_j). \tag{10.14}$$

This additional advantage comes at an elevated computational cost, however. Furthermore, although this approach associates each vector with a scalar value denoting its 'spectral purity', as far as color images are concerned the infimum of a family of vectors calculated in this way corresponds to the notion of median vector. Consequently, it does not carry the significance of a minimum in the numerical sense.

Moreover, if the reference vector is chosen to be 'in the middle' (e.g. the median or the average), the supremum computed by means of these orderings will be very unstable. Indeed, despite the remarkable stability of the infimum under the same conditions, even a slightly varied input can radically change the least upper bound. Consequently, the dilation operator given in equation (10.4) which makes use of the supremum becomes unsound from a practical point of view.

The choice of the distance measure is of course another key topic. Theoretically, any kind of metric can be used; this is the case in practice, with Mahalanobis and Euclidean distances being the most common choices. Observe, however, that any other non-injective transformation can be involved.

In summary, distance-based R-orderings hold the potential for accounting for all dimensions without privileging any of them, a property which becomes particularly useful if there is no predefined order of importance among the available channels (e.g. RGB color images). Otherwise, any transformation capable of realizing the necessary reduction may be used, e.g. a linear-weighted combination [COM 99].

10.3.2.2. *Conditional total pre-orderings*

As previously mentioned, C-orderings restrict the ordering process to only one or more components of the given vectors, while the others are conditioned upon them. That is why C-orderings are suitable for situations where certain channels are more 'privileged' than others. Besides, unless all vector components participate in the ordering process, the resulting C-ordering is bound to be a total pre-ordering (thus sharing their aforementioned inconveniences). For example, in the case where only the first component is employed [HAR 91]:

$$\mathbf{v} \leq \mathbf{v}' \Leftrightarrow v_1 \leq v_1'. \tag{10.15}$$

Hence, the two distinct vectors $\mathbf{a} = [7, 2]^T$ and $\mathbf{b} = [7, 3]^T$ would be considered equivalent according to equation (10.15). The main problem of C-orderings concerns of course the choice of the ordered components. Obviously, ordering vectors along only some of their components is practically justifiable only if the given components sufficiently represent the vectors.

In the general case, this approach attributes far too much significance to the selected components, disregarding all others. While this usually constitutes a severe problem, there are cases where it becomes invaluable: e.g. when it is *a priori* known that certain channels are noise free. In fact, C-orderings are almost always used in combination with a suitable domain space change, so that the data of interest in its majority will lie in only some of the channels.

An example can be found in [VAR 02] where a C-ordering on the HSV color space is employed, ignoring the hue component. This avoids the problem of false

colors, despite the use of a non-total ordering. Specifically, given two HSV triplets $\mathbf{v} = (h, s, v)$ and $\mathbf{v}' = (h', s', v')$:

$$\mathbf{v} \leq \mathbf{v}' \Leftrightarrow \begin{cases} v \leq v', \text{ or} \\ v = v' \text{ and } s \geq s'. \end{cases} \tag{10.16}$$

In fact, this also constitutes a fine example of a combined ordering; more precisely, the result can also be considered as a P-ordering where the ordered groups contain the colors of equal value and saturation with no internal distinction whatsoever, as hue is not taken into account.

10.3.3. *Total orderings*

Total orderings, from a theoretical point of view, have two main advantages that render them more suitable for vector ordering as far as multivariate MM is concerned. First, thanks to their totality, they are vector preserving. Contrary to pre-orderings, as they verify the antisymmetry constraint the computed extrema are unique. That is why the majority of the attempts concentrated on extending morphological operators to multivalued images are based on total orderings. In particular, the lexicographical ordering (C-ordering) along with its variants is among the most implemented choices in color morphology.

However, the uniqueness of extrema takes a serious toll, since the prioritization of certain vector components becomes inevitable [CHA 98]. That is why they are almost always used in combination with a suitable domain transformation (e.g. PCA, a color space with independent components, etc.) that will place the 'interesting' part of the data in the first few channels. Nevertheless, as it will be subsequently presented, some implementations tend to be more 'symmetric' than others.

10.3.3.1. *Lexicographical ordering*

Lexicographical ordering is undoubtedly the most widely employed total ordering within this context, and is defined:

$$\forall \mathbf{v}, \mathbf{v}' \in \mathbb{R}^n, \ \mathbf{v} <_L \mathbf{v}' \Leftrightarrow \exists\, i \in \{1, \ldots, n\}, \ (\forall\, j < i, v_j = v'_j) \wedge (v_i < v'_i). \tag{10.17}$$

We will adopt the notation $V \rightarrow W \rightarrow X$ for vectors in a 3D space VWX where we first compare dimension V, then W and finally X. As a conditional ordering, it is most suitable to situations where an order of importance exists on the available channels, either inherently or artificially created by means of an appropriate transformation. This prioritization of certain vector components with respect to others also constitutes the main drawback of lexicographical ordering, and will be discussed in section 10.4.

To explain, Figure 10.2 provides an example of the priority attributed to the first component during lexicographical ordering. More precisely, a vector dilation is applied to a RGB color image (Figure 10.2, left). As red is the head component, it dominates visibly over green (Figure 10.2, middle). If we permute the channels as GRB, the effect is reversed in favor of green (Figure 10.2, right).

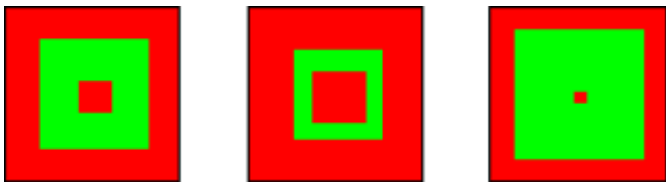

Figure 10.2. *Left: original image. The results of applying a vector dilation based on a lexicographical ordering with a 21 × 21 square SE: RGB (middle) and GRB (right)*

As far as color MM is concerned, the inherent separation of chromatic and achromatic information in color spaces such as $L^*a^*b^*$, HSV and LSH makes lexicographical ordering a prime ordering choice, since achromatic information alone is often sufficient for the recognition of most objects. That is the reason why, unless the application demands it, most color MM implementations are based on brightness-first lexicographical configurations. A first example on the HSV color space can be found in [LOU 02], which however does not take into consideration the 2π periodicity of the hue component [APT 09, HAN 01]. The polar representations of the almost perceptually uniform spaces (e.g. $L^*a^*b^*$ in [HAN 02]) have also been used together with a lexicographical ordering. In addition, following the variety and number of lexicographical approaches developed for phenomenal spaces, Angulo [ANG 05] proposed a 'unified framework' consisting of using the lexicographical ordering in the LSH color space.

10.3.3.2. *Bit mixing based ordering*

Bit interlacing (or mixing) yields an innovative R-ordering, originally developed for RGB color images, mainly aiming to eliminate the unavoidable asymmetry which results from the application of total orderings. Specifically, it employs an injective transformation exploiting the binary representation of each component in order to impose a total order on the vector space [CHA 98].

Given a vector $\mathbf{v}$ with each component coded in k bits, the corresponding reduction transformation $h : \mathbb{Z}^n \rightarrow \mathbb{Z}$ is formulated as:

$$h(\mathbf{v}) = \sum_{m=1}^{k} \left\{ 2^{n(k-m)} \sum_{i=1}^{n} 2^{n-i} v_{i,m} \right\} \tag{10.18}$$

where $v_{i,m}$ denotes the mth bit of the ith component of $\mathbf{v}$. The resulting binary representation of $h(\mathbf{v})$ therefore becomes:

$$v_{1,1}v_{2,1}\ldots v_{n,1}v_{1,2}v_{2,2}\ldots v_{n,2} \quad \ldots \quad v_{1,k}v_{2,k}\ldots v_{n,k}. \tag{10.19}$$

As well as possessing all the qualities of a total ordering, bit mixing provides a more symmetrical approach than its lexicographical counterpart as dimensions are mixed in bit level. Of course, some dimensions continue to be more significant than others, with the degree of that significance being proportional to the significance of the bit position that they occupy. Furthermore, a finer grained symmetry can be obtained by modifying the original mix order [CHA 98]. There are several situations where data channels need to be processed with a certain priority. Bit mixing can easily respond to this requirement by locating the important vector components at more significant bit positions.

Theoretically, this approach aims to fill a given multidimensional space using a balanced *space filling curve* (SFC) with respect to the available dimensions. In the case of total orderings, these curves (e.g. Peano curve) pass through all vector coordinates of the space under consideration, hence vectors can be ordered according to their position on it. More details on SFC will be given in the next section. On the other hand, according to [SOI 02], the main inconvenience of a total ordering obtained in this way is its lack of physical interpretation.

10.3.4. *Synopsis*

This section presented the main approaches that have appeared so far in the literature, with the goal of extending morphological operators to multivalued images. Note that we have omitted some rather unconventional orderings or extremum calculation approaches. These have been excluded since either they do not consist of simply using a standard vector ordering scheme, were developed for a particular form of image data or combine additional theories with the goal of achieving an efficient solution. A more complete description of multivariate mathematical morphology is given in [APT 07].

Unfortunately, each of the main solutions reviewed here posseses a drawback. Partial orderings (or marginal approaches) prevent vector preserving, thus may introduce new (and false) colors or spectral signatures in the resulting image. Pre-orderings do not guarantee extrema uniqueness, which can be a very awkward issue when dealing with morphological operations. Finally, total orderings seem the best solution from a theoretical point of view by avoiding these two drawbacks. However, in practical use, it can be observed that they give importance to the first channel of an image, thus preventing true multivariate image processing. In the following section, we will deal with this problem and present existing and new solutions to ensure symmetry within the most representative total ordering, i.e. lexicographical ordering.

10.4. Balanced total orderings

Lexicographical ordering, defined in equation (10.17), has multiple properties that render it a more adequate choice than its competitors as a way of ordering vectors in the context of multivariate MM. Specifically, the first property is its totality. Since all vectors are lexicographically comparable, it preserves the original vectors of the input image [TAL 98], hence preventing the appearance of false colors. Moreover, as it satisfies the antisymmetry constraint (a property lacking from most reduced orderings), it allows unique vector extrema to be computed, effectively avoiding ambiguities during vector ordering. Additionally, it represents an excellent choice in combination with spaces possessing either an inherent or artificially induced assymetric distribution of information. This is asserted by the number of authors that have considered it, due to its capacity to attribute a certain amount of priority to the first vector or color dimension. That is why it has been popular with phenomenal spaces which effectively separate the different notions of higher level color perception. Additionally, through the control of the channels' order during comparison (e.g. luminance first, saturation second, etc.), it provides a certain degree of customization flexibility. This is a notion of crucial importance as far as general purpose color morphological operators are concerned.

However, notwithstanding its desirable properties, lexicographical ordering also suffers a serious drawback. The outcome of the vast majority of lexicographical comparisons is decided based only on the first few vector components that are compared, while the contribution of its remaining dimensions is typically negligible [HAN 02]. This property is illustrated in Table 10.1, where the percentages of comparisons determined by the three channels of the three RGB color images (Figure 10.3) during a vector dilation based on a lexicographical ordering are listed. The channel occupying the first position of the lexicographical cascade (i.e. red) is obviously responsible for the vast majority of the comparison outcomes.

Images	Equalities (%)	Red (%)	Green (%)	Blue (%)
Lenna	0.12	93.02	6.3	0.56
Macaws	8.89	83.3	5.71	2.1
Mandrill	0.54	95.28	3.51	0.67

Table 10.1. *The percentages of comparisons that have led to equalities and have been determined at each channel during the dilation of the images of Figure 10.3. A lexicographical ordering ($R \rightarrow G \rightarrow B$) using a square-shaped SE of size 5×5 pixels was used*

This might of course be a desired behavior in cases where the fist image channel contains the majority of the total variational information, e.g. after applying a PCA transform. Nevertheless, most often it leads to an insufficient exploitation of the image

(a) (b) (c)

Figure 10.3. *The test images: (a) Lenna, (b) Macaws and (c) Mandrill*

channels and interchannel relations. This effect is most aggravated in the case of hyperspectral images where, despite the availability of hundreds of channels, only the first few at most participate in the overall process. That is why variations of equation (10.17) have been proposed, with the purpose of better tuning the priority as well as degree of influence of each vector component to the comparison outcome.

10.4.1. *Basic solutions to limit asymmetry*

As the majority of lexicographical comparisons are determined by the first components, variants of the classical lexicographical ordering have been proposed with the purpose of better tuning the priority as well as the degree of influence of each component. A first group of variants is based on preceding the lexicographical cascade by a component representative of the entire vector. This principle is used for example along with an Euclidean norm in [RIV 04]:

$$\mathbf{v} \leq \mathbf{v}' \Leftrightarrow [\|\mathbf{v}\|, v_1, \ldots, v_n]^T \leq_L [\|\mathbf{v}'\|, v'_1, \ldots, v'_n]^T \tag{10.20}$$

and similarly in [ANG 07] where a distance with respect to a reference vector is involved (equation (10.13)). Of course, there is no limit to the number or type of functions that can be used according to this principle. Other examples include the use of the maximum and minimum of the compared components in the case of RGB color images, as well as their weighted combinations [ANG 03]. However, these extensions do not provide any way for the user to specify the prioritization among bands.

Another type of extension to the classical lexicographical ordering consists of employing a user-defined parameter α in such a way that it can modify the degree of influence of the first component. The first attempt in this context was made by Ortiz *et al.* [ORT 01], who proposed the α-*lexicographical ordering*:

$$\forall \mathbf{v}, \mathbf{v}' \in \mathbb{R}^n,\ \ \mathbf{v} < \mathbf{v}' \Leftrightarrow \begin{cases} v_1 + \alpha < v'_1, & \text{or} \\ v_1 + \alpha \geq v'_1 & \text{and} \quad [v_2, \ldots, v_n]^T <_L [v'_2, \ldots, v'_n]^T \end{cases}$$

(10.21)

where $\alpha \in \mathbb{R}^+$. The α argument is therefore used after increasing the occurrence of equivalences within the first vector dimension. A scalar value v_1 becomes equal to all values contained in the interval $[v_1 - \alpha, v_1 + \alpha]$, hence allowing comparisons to more frequently reach the second dimension. Nevertheless, equation (10.21) is not transitive, and consequently does not represent an ordering from an algebraic point of view.

A more theoretically sound approach was proposed by Angulo and Serra [ANG 03], referred to as α-*modulus lexicographical ordering*:

$$\forall \mathbf{v}, \mathbf{v}' \in \mathbb{Z}^n, \ \ \mathbf{v} < \mathbf{v}' \Leftrightarrow [\lceil v_1/\alpha \rceil, v_2, \ldots, v_n]^T <_L [\lceil v_1'/\alpha \rceil, v_2', \ldots, v_n']^T \quad (10.22)$$

which aims to create equivalence groups within the first dimension. It relies on a quantization through division by a constant α followed by a rounding off, which reduces the dynamic margin of the first dimension. This allows a greater number of comparisons to reach the second dimension. Contrary to the above-mentioned approach, it is reflexive and transitive hence a pre-ordering.

The effect of the operation applied to the first dimension becomes clearer by studying the *space filling curves* (SFC) that travel through points of multidimensional space. Since the search for a total vector ordering can be formulated as a search for an injective function mapping all the points of a multidimensional space onto a unidimensional space, SFC satisfy this requirement and make it possible to model different solutions. Vectors are ordered according to the position of their coordinates on the SFC.

Since lexicographical ordering corresponds to a bijection [CHA 98], its SFC will pass once on all points of a bidimensional discrete space $D1 \times D2 = [0, 16]^2$ as illustrated in Figure 10.4 (left), where the high priority attributed to the first dimension $(D1)$ is represented by the high frequency of horizontal curves. Figure 10.4 (right) shows the quantized form $D1'$ of dimension $D1$ with $\alpha = 4$, which leads to the creation of equivalence groups. For instance, the points $\{5, 6, 7, 8\}$ of $D1$ now belong to the same group 2 of $D1'$. Given two coordinates $(5, 1)$ and $(7, 0)$ in $D1 \times D2$, the first components are considered equal in $D1' \times D2$ and the outcome of the comparison is determined by the second dimension. In other words, $(5, 1) > (7, 0)$.

Nevertheless, special attention is required with the use of this approach, since the resulting equivalence groups obviously eliminate the antisymmetry property of lexicographical ordering. One way of countering this problem, that renders this approach as well as any other similar to it antisymmetric and thus an ordering, is to continue the lexicographical cascade with the unquantized vector dimensions. To

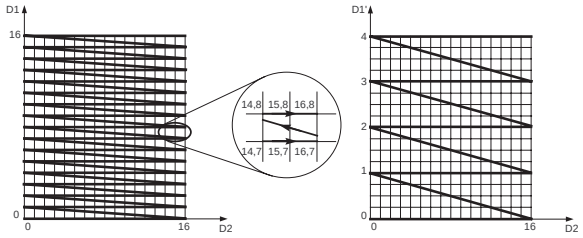

Figure 10.4. *Space filling curves in a bidimensional space for a lexicographical ordering (left) where the arrows denote the direction of increasing vector coordinates, and for the α-modulus lexicographical ordering with $\alpha = 4$ (right)*

explain:

$$\forall\, \mathbf{v}, \mathbf{v}' \in \mathbb{Z}^n,\ \ \mathbf{v} < \mathbf{v}' \Leftrightarrow$$

$$\begin{cases} [j_1(v_1), \ldots, j_{n-1}(v_{n-1}), v_n]^T <_L \left[j_1(v'_1), \ldots, j_{n-1}(v'_{n-1}), v'_n\right]^T, \ \text{or} \\ [j_1(v_1), \ldots, j_{n-1}(v_{n-1}), v_n]^T = \left[j_1(v'_1), \ldots, j_{n-1}(v'_{n-1}), v'_n\right]^T \\ \text{and}\ \ \mathbf{v} <_L \mathbf{v}' \end{cases} \tag{10.23}$$

where $j_i(\cdot), i \in [1, n-1]$ denotes some function used to reduce the dynamic margin of the ith dimension. Only equal vectors are therefore considered equivalent.

In conclusion, among the solutions that have been so far reported with the purpose of fine-tuning the dimension prioritization of lexicographical ordering, only equation (10.22) in combination with equation (10.23) satisfies the theoretical requirements of an ordering and hence leads to valid morphological operators. The practical use of α-modulus lexicographical ordering is however limited, as it relies on an implicit assumption on the dimension to be quantized. In the next section, we present some advanced quantization models which have recently been proposed by the authors [APT 08b, APT 08c].

10.4.2. *Spectral quantization*

As far as its theoretical properties are concerned, α-modulus lexicographical ordering appears to be the most pertinent among the two variations. It provides an effective means of shifting priority away from the first vector dimension, while preserving the desirable characteristics of lexicographical ordering that have made it popular within the color morphological context.

However, its practical use relies upon an important implicit assumption. More precisely, as shown in Figure 10.5a, the dimension under consideration is processed

uniformly. This is based on the assumption that all of its subsets are equally unimportant with respect to the second dimension in the lexicographical cascade. In practice often complicated relations are present among the image channels, and the need to shift priority to the next dimension arises only partially. Consider, for instance, the case of color morphology in a phenomenal color space of type LSH, where the importance of saturation is minimized for extreme levels of luminance.

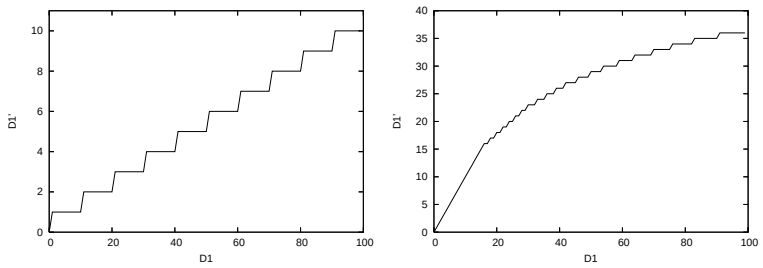

(a) (b)

Figure 10.5. *Example of quantization applied to a dimension D1 using (a)* $\alpha = 10$ *and equation* (10.22)*, and (b) using the proposed approach with the same* α *and an exponential distribution*

Regarding these remarks, we propose the generalization described in algorithm 10.1 as a replacement for the division followed by a rounding off of equation (10.22). Based on a simple principle, this algorithm realizes a quantization of a given discrete pixel range interval in practice, often $I = [0, 255]$, by associating a group of equivalence with each value. The size of this group of equivalence is computed using a user-defined function f, and is limited by the value of $\alpha \in \mathbb{N}^*$. Hence, it is possible to reformulate equation (10.22) as:

$$\forall\, \mathbf{v}, \mathbf{v}' \in \mathbb{Z}^n,\ \ \mathbf{v} < \mathbf{v}' \Leftrightarrow [w_1, v_2, \ldots, v_n]^T <_L [w'_1, v'_2, \ldots, v'_n]^T \qquad (10.24)$$

where w_1 and w'_1 represent the equivalence group of v_1 and v'_1, respectively, obtained through algorithm 10.1. Of course, we are by no means limited to applying this procedure only to the first dimension. In fact, complicated interchannel relations often require the repeated use of such an approach in more than one dimension, in order to be effectively modeled.

Similar to equation (10.22), equation (10.24) also represents a relation lacking the antisymmetry property for the same reasons. That is why we will implicitly consider the combination of equation (10.24) with the standard lexicographical ordering (as shown in equation (10.23)) for tie-breaking purposes.

An example of this algorithm is given in Figure 10.5b, where it is applied to the integer interval $[0, 100]$ using an exponential priority distribution. In other words,

Algorithm 10.1: To compute a quantized discrete dimension based on an arbitrary priority distribution

Input: $I = [a, \ldots, b] \subseteq \mathbb{Z}$, an array containing the discrete dimension to have its dynamic margin reduced
$\alpha \in \mathbb{N}^*$, a parameter setting the maximum allowed size of equivalence groups within I
$f : I \rightarrow [0, 1]$, a function modeling the desired priority distribution within I
Output: $J \subseteq \mathbb{N}$, the array containing the new quantized dimension
$tmp \leftarrow 0$
for $i \leftarrow a$ to b **do**
  $k \leftarrow \lceil \alpha \times f(I[i-a]) \rceil$
  for $j \leftarrow i$ to $i + k$ **do**
    $J[j-a] \leftarrow tmp$
  end for
  $tmp \leftarrow tmp + 1$
  $i \leftarrow i + k$
end for

values close to zero are of high importance and need to be processed with a fine precision, whereas the second dimension may be used with values approaching 100. The increase in the size of equivalence groups can be easily observed as the values approach the upper interval bound. Consequently, in order to obtain the uniform distribution of Figure 10.5a corresponding to the quantization of α-modulus lexicographical ordering with this approach, it is sufficient to employ the constant function $\forall n \in \mathbb{N} : f(n) = 1$ within algorithm 10.1. By using the function f, we can model arbitrary priority distributions within image channels. Furthermore, image-specific ordering approaches may be developed using the histogram of the dimension under consideration (as shown in Figure 10.6), hence leading to adaptive vector orderings.

10.4.3. *Spatial quantization*

Creating artificial equivalence groups within the dimension to reduce its lexicographical priority is an effective means of shifting priority to the remaining vector dimensions. However, this is an operation realized independently from the images to be processed (except if the priority distribution is image specific, e.g. based on its histogram), and no *a priori* information is available on where the (eventually abrupt) equivalence group limits correspond to the input image. This undesirable situation is illustrated in Figure 10.7 where the equivalence groups of a unidimensional discrete signal, obtained from equation (10.22), lead to artificial edges/value variations during comparison.

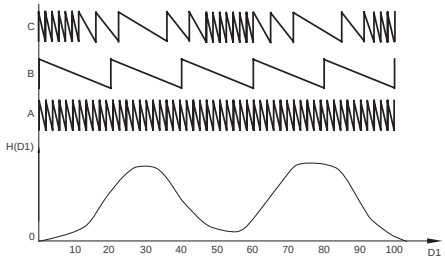

Figure 10.6. *The probability distribution of dimension D1 (bottom) for an arbitrary image, general trend of the space filling curve frequency corresponding to its lexicographical ordering (A),* α*-modulus lexicographical ordering with* $\alpha = 20$ *(B), and quantization-based* α*-lexicographical ordering using the dimension histogram as priority distribution function (C)*

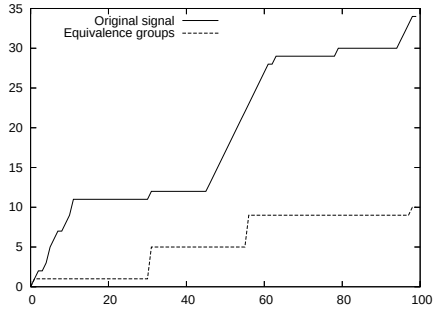

Figure 10.7. *Example of a unidimensional discrete signal with its corresponding equivalence groups, obtained from equation* (10.22) *with* $\alpha = 11$

An alternative way of achieving a priority shift avoiding this inconvenience consists of assuming an image-specific approach and forming these equivalence groups based on the content of the image to be processed. Specifically, we can preprocess the channel of the input image that is to have its priority reduced, so that it is 'flattened' or heavily smoothed. If we call this image a 'marker' m, then the ordering of vectors of an image g can be realized as follows:

$$\forall x, y, s, t \in \mathbb{Z}, \;\; g(x,y) < g(s,t) \Leftrightarrow$$
$$[m(x,y), g_2(x,y), \ldots, g_n(x,y)]^T <_L [m(s,t), g_2(s,t), \ldots, g_n(s,t)]^T . \tag{10.25}$$

In other words, the formation of equivalence groups is now controlled only by the marker image. If a couple of pixels have the same value in the marker image,

then they are considered equal for the dimension that this marker image represents, and the comparison outcome is determined by the following dimensions. Hence equivalence groups are now formed at the flat regions of m (Figure 10.8). The flattening process may be achieved using a variety of filters such as large median filters, alternating sequential filters [SOI 03] or morphological levelings [MEY 04]. Consequently, although the creation of equivalence groups is image specific and needs to be realized independently for each image to be processed, marker-based ordering provides a means of avoiding the artificial edge-related pitfalls of the previously mentioned approaches. The spatial relationships of pixels are taken into account, thus making it possible to accommodate topological restrictions during ordering.

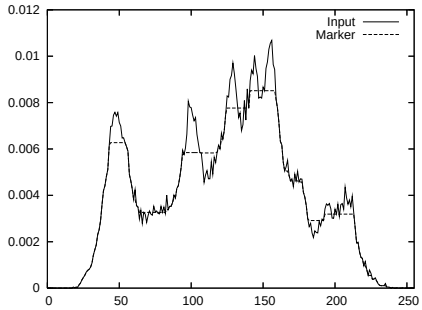

Figure 10.8. *Example of a unidimensional signal and its marker, obtained with an alternating sequential filter using line-shaped SEs of length 5 pixels*

10.4.4. *Iterative quantization*

The third alternative presented here differs greatly from the previous schemes. Instead of considering the problem of color/vector ordering as a means to compute color extrema used for defining the dilation and erosion operators, we concentrate directly on the computation of color extrema given a set of colors. We can therefore exploit the distribution of the vector/color set in the multidimensional space, in order to better control the lexicographical comparison cascade. Naturally, since there is no underlying ordering, there is no complete lattice structure; the resulting operators are therefore theoretically invalid. Nevertheless, as will be shown in section 10.5, they still have a certain practical interest.

10.4.4.1. *Definitions*

The α-trimming principle has long been used in filters such as the α-trimmed mean filter (αMF) and its variants [OTE 04] against impulsive noise. Given a vector $\mathbf{v} \in \mathbb{R}^n$ containing the sorted scalar pixels under the filtering window, the underlying

idea of α-trimming consists of computing their mean by ignoring the 2α extreme:

$$\alpha MF(\mathbf{v}) = \frac{1}{n-2\alpha} \sum_{i=\alpha+1}^{n-\alpha} v_i \tag{10.26}$$

where $\alpha \in [0, n/2]$. In the case of multidimensional vectors, we can apply a similar principle to each dimension in an iterative mode. Specifically, in the case of the maximum, starting from the first dimension we can sort all k vectors according to this dimension and then keep the $\lceil \alpha \times k \rceil$ greatest. By repeating this simple process for each dimension, the initial set of vectors will become smaller at each step. In the eventual case where more than one vector remains at the end of this procedure, the last dimension is used to determine the sought extremum. A more formal description for computing the maximum based on this procedure is given in algorithm 10.2.

Algorithm 10.2: The α-trimmed lexicographical maximum computation algorithm

Input: a set $V = \{v_j\}$ of k, n-dimensional vectors; $\alpha \in]0, 1]$
Output: $\max\ V$
for $i \leftarrow 1$ to $n-1$ **do**
  Sort in increasing order the vectors of V with respect to their ith dimension
  $k \leftarrow \lceil \alpha \times k \rceil$
  $V \leftarrow$ the greatest k vectors in V as well as those equal to the kth vector
  if $(|V| = 1)$ **then**
    return $v \in V$
  end if
  $i \leftarrow i + 1$
end for
return the greatest vector within V with respect to the nth dimension

Similarly, the minimum can be obtained by sorting in a decreasing order. The resulting extrema can therefore be used to define the operators in equations (10.3) and (10.4) for multivariate pixels. An illustration of this approach on a 3D space $D1 \times D2 \times D3$ is given in Figure 10.9. Moreover, the advantage of a collective extremum calculation is accompanied by an increased computational burden. Assuming an optimal sorting procedure is used where all n dimensions would need to be sorted, the complexity would be of the order $O(n \times k \times \log k)$ in the worst scenario with k vectors. On the other hand, with the standard lexicographical ordering and the same scenario, the complexity would be $O(n \times k)$. Note that since k represents the size of the SE in use, its value is relatively small.

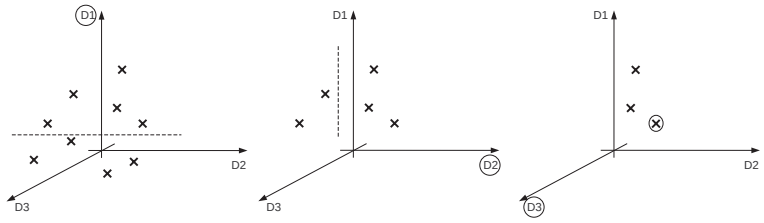

Figure 10.9. *A set of vectors in a 3D space $D1 \times D2 \times D3$, and the three iterations of the α-trimmed lexicographical maximum computation with $\alpha = 0.5$ (left to right). According to the proposed approach, the maximum is the greatest for the third dimension of the remaining three vectors*

10.4.4.2. *Setting α*

The extrema obtained in this way depend directly on the value of α. As a matter of fact, with an α approaching 0 from each dimension i, only the extreme (i.e. maximum or minimum) vector is kept along with those equal to it with respect to the ith dimension. In other words, the procedure becomes identical to the standard lexicographical ordering. On the other hand, when α approaches 1, priority is gradually shifted to the last dimension, and almost all initial vectors reach the last dimension where the comparison is finally decided.

This transition of priority is illustrated in Figure 10.10. When keeping only a single value at each dimension, identically to a standard lexicographical ordering, the first dimension determines the outcome of the majority of comparisons. The final decision is shifted rapidly to the last dimension by slightly increasing the number of kept vectors. The main difference with respect to other lexicographical ordering approaches is the collective extremum calculation, conversely to a binary calculation. Even if the final extremum choice is made in the last dimension, unless $\alpha = 1.0$ all previous dimensions contribute to this choice by trimming the set of vectors accordingly. Additionally, more complicated priority relations among the available channels can be established by means of different α values for each vector dimension.

In practice however, it is often necessary to set these arguments in an unsupervised way. Here we introduce a simple parameter-setting model based on the standard deviation (σ) of each dimension. More precisely, if the data are relatively concentrated with respect to their ith dimension or (in other words) if this image channel does not contain much of the total variational information, we consider a larger α to be more pertinent. This would reduce the influence of this dimension by carrying the majority of the input to the next dimension with minor trimming. On the other hand, if the data are highly dispersed with respect to the other dimensions (meaning that this channel represents relatively important variational information), a small α would be used leading to major trimming. Given n dimensions, one way of obtaining the

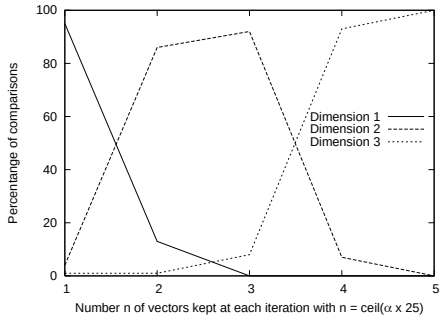

Figure 10.10. *The plot of comparisons decided by each dimension of the image Lenna (Figure 10.3a) in the RGB color space during a dilation with a square-shaped SE of size* 5×5 *pixels, for various numbers of vectors kept at each iteration*

corresponding α_i value of dimension i would be:

$$\forall\, i \in \{1, \ldots, n\}\,,\ \ \alpha_i = 1 - \frac{\sigma_i}{\sum_{j=1}^{n} \sigma_j} \tag{10.27}$$

where σ_j denotes the standard deviation of dimension j. A more effective way of employing this principle would be to first apply a principal components transformation on the image data and then use the variances of each new dimension to this end.

10.4.4.3. *Variations*

Using the α argument as a cardinality limit at each iteration of the algorithm can lead to unexpected situations, such as that shown in Figure 10.11. Indeed, by selecting the vectors to be used in the next stage of the cascade based only on the cardinality of the vector set (i.e. $\lceil \alpha \times k \rceil$) (in other words, irrespectively of their relative distances), we may end up with extremely scattered vector clusters. This situation can be easily countered by using α as a distance measurement. Instead of keeping the $\lceil \alpha \times k \rceil$ greatest vectors with respect to the ith dimension, we can only keep the vectors whose ith dimension is at most at distance α with respect to the greatest vector of the same dimension.

A more important disadvantage of α-trimmed lexicographical extrema is the lack of an underlying binary ordering relation, as previously mentioned. Nevertheless, given any extremum computation method, it is possible to construct an ordering from it. In particular, considering a discrete multidimensional space, we can employ the collective extremum computation method at hand in order to calculate the maximum or minimum of this space. We then repeat for the remaining points until the entire space is ordered.

Moreover, since α-trimmed lexicographical extrema are unique, this approach leads to a total ordering. The exact algebraic properties of the result depend strongly

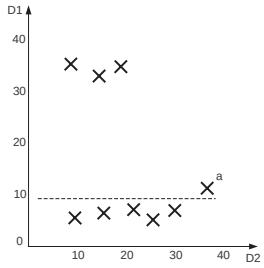

Figure 10.11. *Example of problematic vector distribution. The vector* ***a*** *is chosen as maximum with* $\alpha = 0.4$*, while being positioned at a far distance with respect to the upper vector group*

on both the extremum computation method used (e.g. α-trimmed lexicographical, cumulative distances, etc.) as well as on the extremum employed (i.e. minimum or maximum) during its construction.

10.5. Application to color image analysis: texture classification

Having provided an insight into several morphological frameworks and some recent improvements over lexicographical ordering, we now conduct a series of comparative tests with the aim of better determining their properties and relative performances. Since a representative application for which effective means of quantitative performance assessment are available, we focus on the problem of color texture classification and employ the color textures of Outex13 (Figure 10.12) [OJA 02]. This set contains 68 different textures with 20 images, each obtained with 100 dpi resolution under an incandescent CIE A light source. The total number of 1,360 images have been evenly divided as training and test sets.

The question of whether color should be processed separately from or jointly with texture is still an open problem [MAE 04]; vector morphological feature extraction operators represent in their majority the latter case [HAN 05]. As a color texture descriptor we employ the morphological version of the autocorrelation operator, namely morphological covariance which was initially proposed [MAT 75, SER 82] as the equivalent in MM of the autocorrelation operator. The morphological covariance K of an image f is defined as the volume Vol (i.e. sum of pixel values for gray-level images, sum of the Euclidean norm of pixels in RGB for color images, etc.), of the image, eroded by a pair of points $P_{2,v}$ separated by a vector v:

$$K(f; P_{2,v}) = \mathrm{Vol}\left(\varepsilon_{P_{2,v}}(f)\right). \tag{10.28}$$

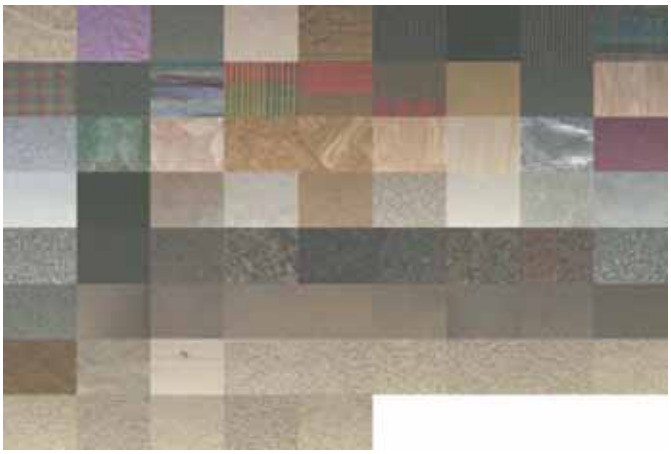

Figure 10.12. *Examples of the 68 textures of Outex 13 [MAE 04]*

In practice, K is computed for varying lengths of **v** and the normalized version is used most often for measurements:

$$K^n(f) = \mathrm{Vol}\left(\varepsilon_{P_{2,v}}(f)\right) / \mathrm{Vol}\,(f)\,. \tag{10.29}$$

Given the resulting unidimensional covariance series, we can gain insight into the structure of a given image [SOI 03]. In particular, the periodic nature of covariance is strongly related to that of its input. Furthermore, the period of periodic textures can easily be determined by the distance between the repeated peaks that appear at multiples of the sought period. The size of the periodic pattern can be quantified by means of the width of the peaks. In other words, their sharpness is directly proportional to the thinness of the texture patterns appearing in the input. Likewise, the initial slope at the origin provides an indication of the coarseness, with quick drop-off corresponding to coarse textures. In order to obtain additional information on the directionality of f, we can not only plot covariance against different lengths of **v** but also against orientations.

The covariance-based feature vectors have been calculated using four directions for the point pairs (0, 45, 90 and 135°), each with distances ranging from 1 to 49 pixels in steps of 2. Consequently, 25 values are available for each direction, making a total of 100 values for every image channel after concatenation. The classification process is realized using a kNN classifier with $k = 1$ [MAE 04]. The color space under consideration is LSH [ANG 05].

In order to carry out the various quantization steps, the luminance channel is manipulated with integer precision in $[0, 255]$. In particular, the extrema employed for defining the basic morphological operators are computed using:

– only the luminance channel (Lum),

– only the saturation (Sat),

– only hue (Hue),

– lexicographical ordering, equation (10.17) (Lex),

– α-modulus lexicographical ($\alpha = 10$), equation (10.22) (α-modLex),

– quantization-based α-lexicographical ($\alpha = 10$), equation (10.24) (QuantaLex) (the LSH prioritization function f described in [APT 08c]),

– the marker-based lexicographical ordering, equation (10.25) (MarkerLex) (where the marker image is obtained by applying a leveling [MEY 04] along with a leveling marker image provided by median filtering with a square-shaped SE of size 7×7),

– the α-trimmed lexicographical extrema ($\alpha = 0.45$) (α-trimmedLex) according to algorithm 10.2 as well as its variations (using adaptive α values or by equation (10.27)) (α-trimmedLex-adaptive),

– the total ordering resulting from the application of collective extremum computation scheme with $\alpha = 0.45$ (α-trimmedLex-ordering), and

– the version based on distance computations with $\alpha = 0.3$.

The comparisons are realized in the order $L \rightarrow S \rightarrow H$, and the hue component is processed according to the principle of weighted multiple references (not described here; see [APT 09]).

The results obtained from this texture classification application are given in Table 10.2. The overall performances appear to be relatively close. Specifically, the pertinence of luminance over both saturation and hue is observed, showing that color information is in this case just an auxiliary component. As expected, Lum and Lex exhibit almost identical performances, a result showing the level of priority attributed to the first component (largely ignoring the remaining two dimensions). A minor improvement over Lex is obtained through α-modLex, as it allows saturation to participate at a slightly higher degree in the process of computing covariance. However, hue remains largely unexploited. With the use of α-trimmed extrema, the chrominance dimensions increase their contribution to the final result. As a matter of fact, the empirically set α-trimmedLex leads to an overall best, while the unsupervised model provides a relatively sufficient approximation. Nevertheless, no improvements are observed with the last two variations. Moreover, QuantaLex leads to an improvement over α-modLex, as it controls the transitions among the image channels in a finer way (the difference, however, being almost negligible). The marker-based approach improves the spectral quantization-based ordering substantially and

outperforms α-modLex. Apparently, the use of saturation with relatively 'flat' regions and that of luminance with transitions within the image lead to more pertinent descriptors by combining color and textural information in a better way.

	Accuracy (%)
Lum	73.82
Sat	66.91
Hue	55.29
Lex	74.26
α-modLex	76.62
QuantaLex	77.17
MarkerLex	79.86
α-trimmedLex	**81.47**
α-trimmedLex-adaptive	79.89
α-trimmedLex-ordering	54.35
α-trimmedLex-distance	73.74

Table 10.2. *Classification accuracies for the textures of Outex13 using vector erosion-based covariance*

10.6. Conclusion

This chapter has introduced the theoretical concepts behind the multivariate morphological framework, as well as the various approaches that have been proposed with this purpose. Given the complete lattice theory-based structure of morphology, it becomes easy to observe that a vector ordering is sufficient for the definition of valid multivariate morphological operators. Among the numerous ordering possibilities, total orderings are the most theoretically sound approaches since they ensure extrema uniqueness and vector preservation.

In this context, the lexicographical ordering is certainly the most widely used total ordering since, as well as the previously mentioned theoretical advantages, it also provides a means of effective customization through the configuration of the order of the lexicographical cascade. However, its standard definition introduces an extreme prioritization of the first vector dimension and thus limits its practical interest by ignoring the other available image channels.

We address this problem and present three different variations of lexicographical ordering with the purpose of resolving this issue. The first, quantization-based α-lexicographical ordering, consists of a generalization of the α-modulus ordering. Sub-quantizing the vector dimensions according to arbitrary models enables the user to incorporate into the ordering any *a priori* information available on the channels under consideration. The second variation of lexicographical ordering,

marker-based lexicographical ordering, uses an image-specific principle. The first channel is processed by means of gray-level operators in order to form flat zones that determine the areas where priority is shifted to the subsequent dimensions. Additionally, a third method for computing α-trimmed lexicographical extrema has been introduced, which also succeeds in manipulating the contribution of each channel to this process through a user-defined argument. Nevertheless, as there is no underlying ordering it leads to pseudo-morphological color operators.

A comparison between the different vector orderings presented in this chapter has also been given, with the purpose of texture classification in color images by means of morphological covariance. Nevertheless, it should be noted that the proposed ordering variations are usable in the general case of multivariate image data, e.g. hyperspectral remote sensing images or multispectral astronomical images.

Further reading related to multivariate mathematical morphology applied to color image analysis includes [APT 07, APT 08a, APT 08b, APT 08c, APT 09], as well as the numerous work carried out at the leading research center within the field of mathematical morphology, namely the *Centre de Morphologie Mathématique* of the Mines ParisTech School, France (see http://cmm.ensmp.fr).

10.7. Bibliography

[ALO 03] AL-OTUM H. M., "Morphological operators for color image processing based on Mahalanobis distance measure", *Optical Engineering*, vol. 42, num. 9, p. 2595–2606, September 2003.

[ANG 03] ANGULO J., SERRA J., "Morphological coding of color images by vector connected filters", *IEEE Proceedings of the 7th International Symposium on Signal Processing and its Applications (ISSPA'2003)*, vol. 1, Paris, France, p. 69–72, July 2003.

[ANG 05] ANGULO J., "Unified morphological color processing framework in a lum/sat/hue representation", RONSE C., NAJMAN L., DECENCIÈRE E., Eds., *Mathematical Morphology: 40 Years On*, vol. 30 of *Computational Imaging and Vision*, p. 387–396, Springer-Verlag, Dordrecht, 2005.

[ANG 07] ANGULO J., "Morphological colour operators in totally ordered lattices based on distances: Application to image filtering, enhancement and analysis", *Computer Vision and Image Understanding*, vol. 107, num. 1–2, p. 56–73, July 2007.

[APT 07] APTOULA E., LEFÈVRE S., "A comparative study on multivariate mathematical morphology", *Pattern Recognition*, vol. 40, num. 11, p. 2914–2929, November 2007.

[APT 08a] APTOULA E., Analyse d'images couleur par morphologie mathématique. Application à la description, l'annotation, et la recherche d'images – colour image analysis with mathematical morphology. Application to image description, annotation, and retrieval, PhD thesis, Louis Pasteur University, Strasbourg, France, 2008.

[APT 08b] APTOULA E., LEFÈVRE S., "Alpha-trimmed lexicographical extrema for pseudo-morphological image analysis", *Journal of Visual Communication and Image Representation*, vol. 19, num. 3, p. 165–174, April 2008.

[APT 08c] APTOULA E., LEFÈVRE S., "On lexicographical ordering in multivariate mathematical morphology", *Pattern Recognition Letters*, vol. 29, num. 2, p. 109–118, January 2008.

[APT 09] APTOULA E., LEFÈVRE S., "On the morphological processing of hue", *Image and Vision Computing*, vol. 27, num. 9, p. 1394–1401, 2009.

[AST 90] ASTOLA J., HAAVISTO P., NEUVO Y., "Vector median filters", *IEEE Proceedings*, vol. 78, num. 4, p. 678–689, April 1990.

[BAR 76] BARNETT V., "The ordering of multivariate data", *Journal of the Statistical Society A*, vol. 139, num. 3, p. 318–355, 1976.

[CHA 98] CHANUSSOT J., Approches vectorielles ou marginales pour le traitement d'images multi-composantes, PhD thesis, University of Savoie, France, 1998.

[COM 99] COMER M., DELP E., "Morphological operations for color image processing", *Journal of Electronic Imaging*, vol. 8, num. 3, p. 279–289, July 1999.

[GOU 95] GOUTSIAS J., HEIJMANS H. J. A. M., SIVAKUMAR K., "Morphological operators for image sequences", *Computer Vision and Image Understanding*, vol. 62, num. 3, p. 326–346, November 1995.

[GOU 00] GOUTSIAS J., HEIJMANS H. J. A. M., "Fundamenta morphologicae mathematicae", *Fundamenta Informaticae*, vol. 41, num. 1–2, p. 1–31, January 2000.

[HAN 01] HANBURY A., SERRA J., "Morphological operators on the unit circle", *IEEE Transactions on Image Processing*, vol. 10, num. 12, p. 1842–1850, December 2001.

[HAN 02] HANBURY A., SERRA J., "Mathematical morphology in the CIELAB space", *Image Analysis and Stereology*, vol. 21, num. 3, p. 201–206, March 2002.

[HAN 05] HANBURY A., KANDASWAMY U., ADJEROH D. A., "Illumination-invariant morphological texture classification", RONSE C., NAJMAN L., DECENCIÈRE E., Eds., *Mathematical Morphology: 40 Years On*, vol. 30 of *Computational Imaging and Vision*, p. 377–386, Springer-Verlag, Dordrecht, 2005.

[HAN 08] HANBURY A., "Constructing cylindrical coordinate colour models", *Pattern Recognition Letters*, vol. 4, num. 29, p. 494–500, March 2008.

[HAR 91] HARDIE R. C., ARCE G. R., "Ranking in R^p and its use in multivariate image estimation", *IEEE Transactions on Circuits and Systems for Video Technology*, vol. 1, num. 2, p. 197–209, June 1991.

[HEI 90] HEIJMANS H. J. A. M., RONSE C., "The algebraic basis of mathematical morphology, part I: dilations and erosions", *Computer Vision, Graphics and Image Processing*, vol. 50, num. 3, p. 245–295, June 1990.

[HEI 94] HEIJMANS H. J. A. M., *Morphological Image Operators*, Advances in Electronics and Electron Physics Series, Academic Press, Boston, 1994.

[LOU 02] LOUVERDIS G., VARDAVOULIA M., ANDREADIS I., TSALIDES P., "A new approach to morphological color image processing", *Pattern Recognition*, vol. 35, num. 8, p. 1733–1741, September 2002.

[MAE 04] MAENPAA T., PIETIKAINEN M., "Classification with color and texture: jointly or separately?", *Pattern Recognition*, vol. 37, num. 8, p. 1629–1640, 2004.

[MAT 75] MATHERON G., *Random Sets and Integral Geometry*, Wiley, New York, 1975.

[MEY 04] MEYER F., "Levelings, image simplification filters for segmentation", *Journal of Mathematical Imaging and Vision*, vol. 20, p. 59–72, 2004.

[OJA 02] OJALA T., MAENPAA T., PIETIKAINEN M., VIERTOLA J., KYLLONEN J., HUOVINEN S., "Outex: New framework for empirical evaluation of texture analysis algorithms", *Proceedings of the 16th ICPR*, vol. 1, Quebec City, Canada, p. 701–706, August 2002.

[ORT 01] ORTIZ F., TORRES F., ANGULO J., PUENTE S., "Comparative study of vectorial morphological operations in different color spaces", *Proceedings of Intelligent Robots and Computer Vision XX: Algorithms, Techniques, and Active Vision*, vol. 4572, p. 259–268, November 2001.

[OTE 04] OTEN R., DE FIGUEIREDO R. J. P., "Adaptive alpha-trimmed mean filters under deviations from assumed noise model", *IEEE Transactions on Image Processing*, vol. 13, num. 5, p. 627–639, May 2004.

[PLA 04] PLAZA A., MARTINEZ P., PEREZ R., PLAZA J., "A new approach to mixed pixel classification of hyperspectral imagery based on extended morphological profiles", *Pattern Recognition*, vol. 37, num. 6, p. 1097–1116, June 2004.

[RIV 04] RIVEST J., "Morphological operators on complex signals", *Signal Processing*, vol. 84, num. 1, p. 133–139, January 2004.

[RON 91] RONSE C., HEIJMANS H. J. A. M., "The algebraic basis of mathematical morphology, part II: openings and closings", *Computer Vision, Graphics and Image Processing*, vol. 54, num. 1, p. 74–97, July 1991.

[SER 82] SERRA J., *Image Analysis and Mathematical Morphology Vol I*, Academic Press, London, 1982.

[SER 93] SERRA J., "Anamorphoses and function lattices", DOUGHERTY E. R., Ed., *Mathematical Morphology in Image Processing*, Chapter 13, p. 483–523, Marcel Dekker, New York, 1993.

[SER 05] SERRA J., "Morphological segmentations of colour images", RONSE C., NAJMAN L., DECENCIÈRE E., Eds., *Mathematical Morphology: 40 Years On*, vol. 30 of *Computational Imaging and Vision*, p. 151–176, Springer-Verlag, Dordrecht, 2005.

[SOI 02] SOILLE P., PESARESI M., "Advances in mathematical morphology applied to geoscience and remote sensing", *IEEE Transactions on Geoscience and Remote Sensing*, vol. 40, num. 9, p. 2042–2055, September 2002.

[SOI 03] SOILLE P., *Morphological Image Analysis: Principles and Applications*, Springer-Verlag, Berlin, 2nd edition, 2003.

[TAL 98] TALBOT H., EVANS C., JONES R., "Complete ordering and multivariate mathematical morphology", HEIJMANS H., ROERDINK J., Eds., *Mathematical Morphology and its Applications to Image and Signal Processing*, Amsterdam, Kluwer Academic Press, p. 27–34, 1998.

[VAR 02] VARDAVOULIA M. I., ANDREADIS I., TSALIDES P., "Vector ordering and morphological operations for colour image processing: fundamentals and applications", *Pattern Analysis and Applications*, vol. 5, num. 3, p. 271–287, 2002.

[WIL 92] WILSON S. S., "Theory of matrix morphology", *IEEE Transactions on Pattern Analysis and Machine Intelligence*, vol. 14, num. 6, p. 636–652, June 1992.